

Supplementary Information

## Reasons Behind the Improved Thermoelectric Properties of Poly(3-hexylthiophene) Nanofiber Networks

Balázs Endródi, János Mellár, Zoltán Gingl, Csaba Visy, and Csaba Janáky\*

### Details of the experimental procedures

#### Materials

All chemicals were from commercial sources and were of highest available purity. 3-hexylthiophene (Sigma-Aldrich), anhydrous  $\text{FeCl}_3$  (VWR), absolute ethanol (Molar), tetrahydrofuran (Molar), anisole (Fluka) and anhydrous  $\text{AgClO}_4$  (Sigma-Aldrich) were used as received. Water content of nitrobenzene (Sigma-Aldrich) and chloroform (Carlo-Erba) solvents was kept below 50 ppm using 3A zeolites (Sigma-Aldrich).

#### Synthesis

Poly(3-hexylthiophene) (P3HT) was prepared by oxidative chemical polymerization:<sup>1</sup> chloroform based 3-hexylthiophene and  $\text{FeCl}_3$  solutions were mixed at final reagent concentrations of 0.1 and 0.25 M, respectively. The continuously stirred reaction mixture was kept in a closed vessel on ice bath for 6 hours. To remove the traces of the oxidant, the precipitated P3HT was washed repeatedly with ethanol. The final product was dried in air, at room temperature.

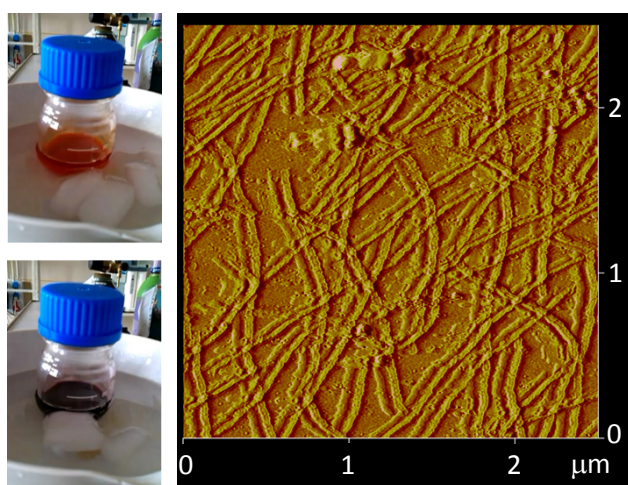


**Figure S1.** (a) Color change of the P3HT solution upon recrystallization (b) AFM image of the drop-casted P3HT nanonet

Whisker method was employed to form nanofibers from the bulk polymer. First the larger molecular weight fraction of P3HT was Soxhlet extracted by tetrahydrofuran (THF). After evaporating the solvent, the polymer was re-dissolved in 9:1 ratio anisole/chloroform solvent to get final polymer concentration of  $2.5 \text{ g dm}^{-3}$ . The solution was heated to  $70 \text{ }^\circ\text{C}$  and then instantly cooled down to room temperature on ice bath. During the recrystallization process, color of the solution changed from orange to dark purple (Figure S1).

AFM studies provided further evidence on the successful recrystallization process: as depicted in Figure S1, AFM images revealed the presence of 50-60 nm wide and several micrometer long, randomly oriented P3HT nanofibers, forming a coherent network (nanonet).

Thin films of the P3HT nanofibers (nanonets) were formed by drop casting  $400 \text{ }\mu\text{l}$  of the solution on plastic substrates ( $2 \text{ cm} \times 2.5 \text{ cm}$ ). These plastic sheets were previously patterned with 4 gold stripes ( $1 \text{ mm}$  wide,  $25 \text{ mm}$  long, and  $1 \text{ mm}$  spatial interval) for 4 point probe electrical measurements. For comparison, non-fibrillar films were formed similarly, from toluene based solution ( $2.5 \text{ g dm}^{-3}$ ) of the chemically prepared P3HT.

For the successful doping procedure, the optimal solvent must fulfil several requirements, including proper polymer wetting, solubility of the oxidant, and insolubility of the polymer. After performing experiments with a number of different solvents (water, acetone, acetonitrile, toluene, propylene-carbonate, and N,N-dimethyl formamide) nitrobenzene was the only one which met *all* the above requirements, and was chosen for all later experiments.

## Characterization

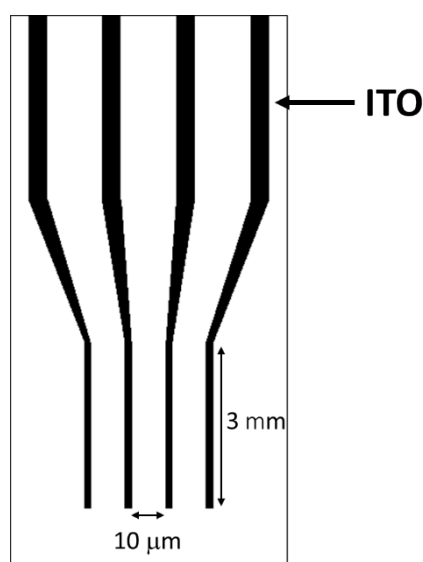


**Figure S2.** Scheme of the special ITO coated electrode, used for in situ spectroelectrochemical studies

During the simultaneous in situ spectral and impedance measurements, a special indium tin oxide (ITO)-coated glass working electrode (IAME, Abtech) was employed. It consisted of  $5 \text{ }\mu\text{m}$  wide and  $3$

mm long needles, forming gaps of 10  $\mu\text{m}$  width between the neighboring electrode parts (Figure S2). P3HT was drop-casted on this substrate to form electrical contact between the needles, so conductance can be measured. The ITO-covered glass support makes optical transmission measurements possible. *In situ* UV-Visible-near infrared spectroscopic measurements were carried out, using an Agilent 8453 UV-visible diode array spectrophotometer in the 430–1100 nm wavelength range. Data obtained from AC impedance measurements at 130 Hz were analyzed by a lock-in amplifier (SR 830) (See Reference 20 in the m/s).

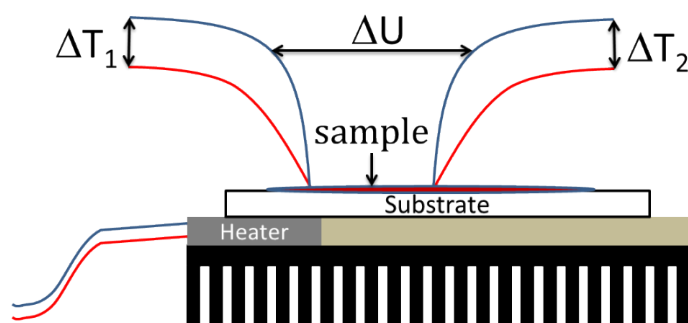


**Figure S3.** Scheme of the custom built setup, used to measure the Seebeck coefficient

Thermoelectric characterization was carried out using a custom designed measurement setup (Figure S3).<sup>2</sup> Temperature gradient – formed by heating the sample with a Peltier-heater, by applying constant heating power – was measured quasi-continuously (13392 Hz sampling frequency) by two J-type thermocouples, connected to a FES24 type data acquisition unit. Simultaneously, potential difference was registered by the same probes, by connecting the positive wires of the thermocouples to a 3<sup>rd</sup> channel of the instrument. The setup was validated by measuring the Seebeck coefficient of standard p- and n-type  $\text{Bi}_2\text{Te}_3$  samples. Electrical conductivity of the samples was determined by 4 point probe method, using a Keithley 2400 type general purpose source meter.

## Results and Discussions

### UV-Vis spectroscopy of the P3HT samples

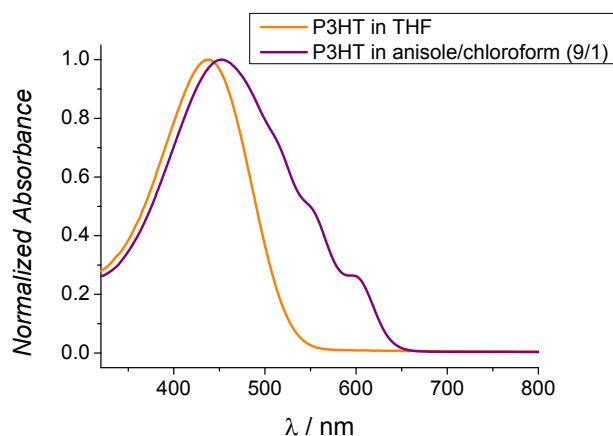


**Figure S4.** Changes on the UV-Vis spectrum of P3HT during the recrystallization process

The recrystallization procedure is accompanied by the red shift of UV-Visible absorption maximum from  $\lambda_{\text{max}}=438$  to 452 nm when the solvent was changed from pure tetrahydrofuran to 9/1 ratio anisole/chloroform mixture. Importantly, appearance of the fine vibronic structure ( $\pi$ - $\pi^*$  absorption bands at 508, 550, and 592 nm) is a clear indication on the nanofiber formation.<sup>3-5</sup>

### FTIR study of the P3HT nanonet

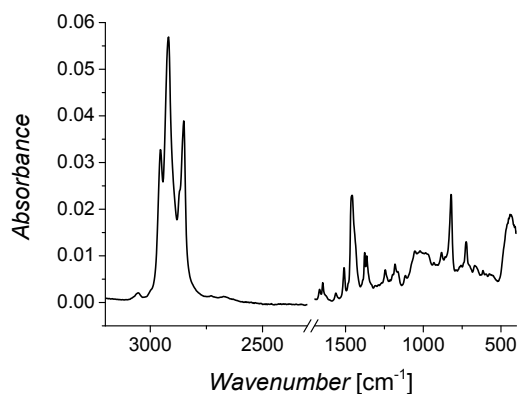


**Figure S5.** FT-IR spectrum of the P3HT nanonet in its neutral form

| $\nu / \text{cm}^{-1}$ | Vibration mode                                  |
|------------------------|---|
| 724                    | C-H out-of-plane vibration                      |
| 821                    |   |
| 1052                   | C-H in-plane vibration                          |
| 1377                   | -CH <sub>3</sub> deformational vibration        |
| 1459                   | C=C symmetric stretching                        |
| 1510                   | C=C antisymmetric stretching                    |
| 2851                   | Symmetric C-H stretching in -CH <sub>2</sub> -  |
| 2919                   | Asymmetric C-H stretching in -CH <sub>2</sub> - |
| 2954                   | Asymmetric C-H stretching in -CH <sub>3</sub> - |
| 3055                   | Aromatic C-H stretching                         |

**Table S1.** Characteristic vibrations of the P3HT nanonet <sup>6,7</sup>

Infrared spectrum (Figure S5) of the P3HT nanonet is consistent with other P3HT materials published earlier. Three characteristic regions of the spectrum around 3000, 1500 and 800  $\text{cm}^{-1}$  can be attributed to the C-H vibration of the alkyl side-chain, the vibration of the thiophene ring and the in- and out-of-plane vibrations of the aromatic C-H groups, respectively (Table S1).

Importantly, the position of the aromatic C-H out-of-plane vibration ( $821 \text{ cm}^{-1}$ ), shifted to lower wavenumbers ( $820\text{-}822 \text{ cm}^{-1}$ ), which is typical for regioregular poly(3-alkylthiophene)s (See Reference 22 in the m/s).

#### *Structure of the doped P3HT nanonet*

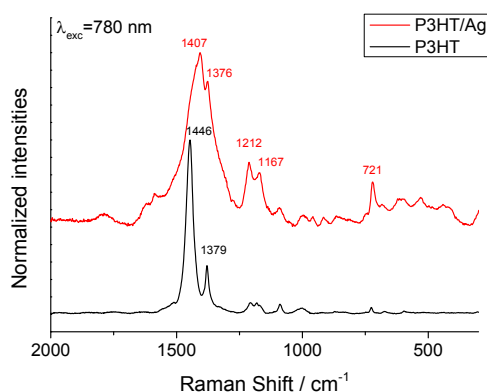


**Figure S6.** Raman spectra of the undoped and the Ag<sup>+</sup> doped ([AgClO<sub>4</sub>] $\sim$ 25mM) P3HT nanonet

Raman spectrum (Figure S7) of the undoped and silver doped P3HT nanonet is consistent with other P3HT materials published earlier (see reference 23 in the m/s). The changes in the relative intensities of peaks related to C <sub>$\alpha$</sub> -S-C <sub>$\alpha$</sub> ' deformation ( $721 \text{ cm}^{-1}$ ) and C <sub>$\alpha$</sub> -C <sub>$\alpha$</sub> ' stretching vibration ( $1212 \text{ cm}^{-1}$ ,

characteristic to the head-to-tail structure), and shift of the band at  $1446\text{ cm}^{-1}$  (related to the  $C_{\alpha}=C_{\beta}$  stretching) to significantly lower wavenumber (energy), to  $1407\text{ cm}^{-1}$ , confirm the presence of a heavily doped form of the P3HT nanonet.

#### Analysis of XRD data

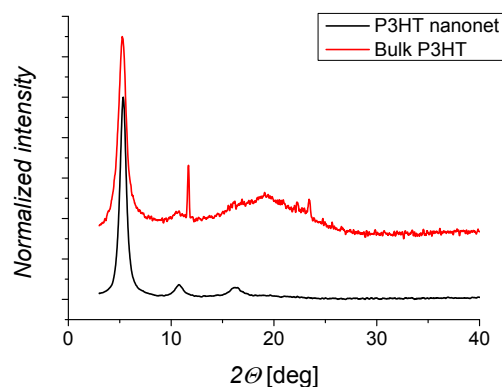


**Figure S7.** XRD diffractograms of the P3HT nanonet and the non-fibrillar P3HT

The two sharp diffraction on the XRD pattern of the non-fibrillar P3HT (Figure S6) at  $2\Theta=5.24$  and  $23.42^\circ$  ( $16.85$  and  $3.795\text{ \AA}$ ) are related to the distance between the side-chain interdigitated, and the  $\pi$ -stacked polymer chains, respectively. The relatively low intensity hill-type reflection between  $2\Theta=14-27^\circ$  indicates the presence of an amorphous P3HT phase.

Contrarily, the P3HT nanonet shows sharp reflections *only*, instead of broad, hill-type reflection (typically observed for regiorandom P3HT obtained by chemical polymerization). This can be attributed to a highly-ordered structure, in which the individual chains are stacked together by the interaction of the overlapping aromatic rings ( $\pi$ -stacking) and the zipper like connection of the alkyl side chains. Note, that the reflection expected  $2\Theta^\circ = 23.4$  is absent in the case of the nanonet. This can be attributed its supramolecular structure: the P3HT nanofibers are orientated in the  $\pi-\pi$  stacking direction in plane of the film.<sup>4</sup>

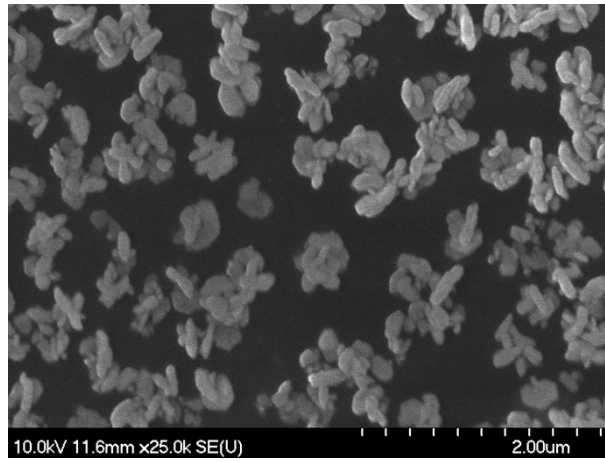


**Figure S8.** SEM image of the Ag<sup>+</sup> doped ([AgClO<sub>4</sub>]<sub>~25mM</sub>) P3HT nanonet

SEM images taken at different magnifications furnished several important insights, verifying and expanding the conclusions derived from TEM experiments. Most importantly: (i) Ag appears as 4-600 nm large silver agglomerates – formed by 50-200 nm sized nanoparticles – at the highest AgClO<sub>4</sub> concentration (ii) distribution of the silver particles is uniform on the whole P3HT nanonet (iii) the deposited Ag particles do not form a percolation pathway through the bulk nanonet structure.

*Thermoelectric properties of silver doped P3HT nanonets*

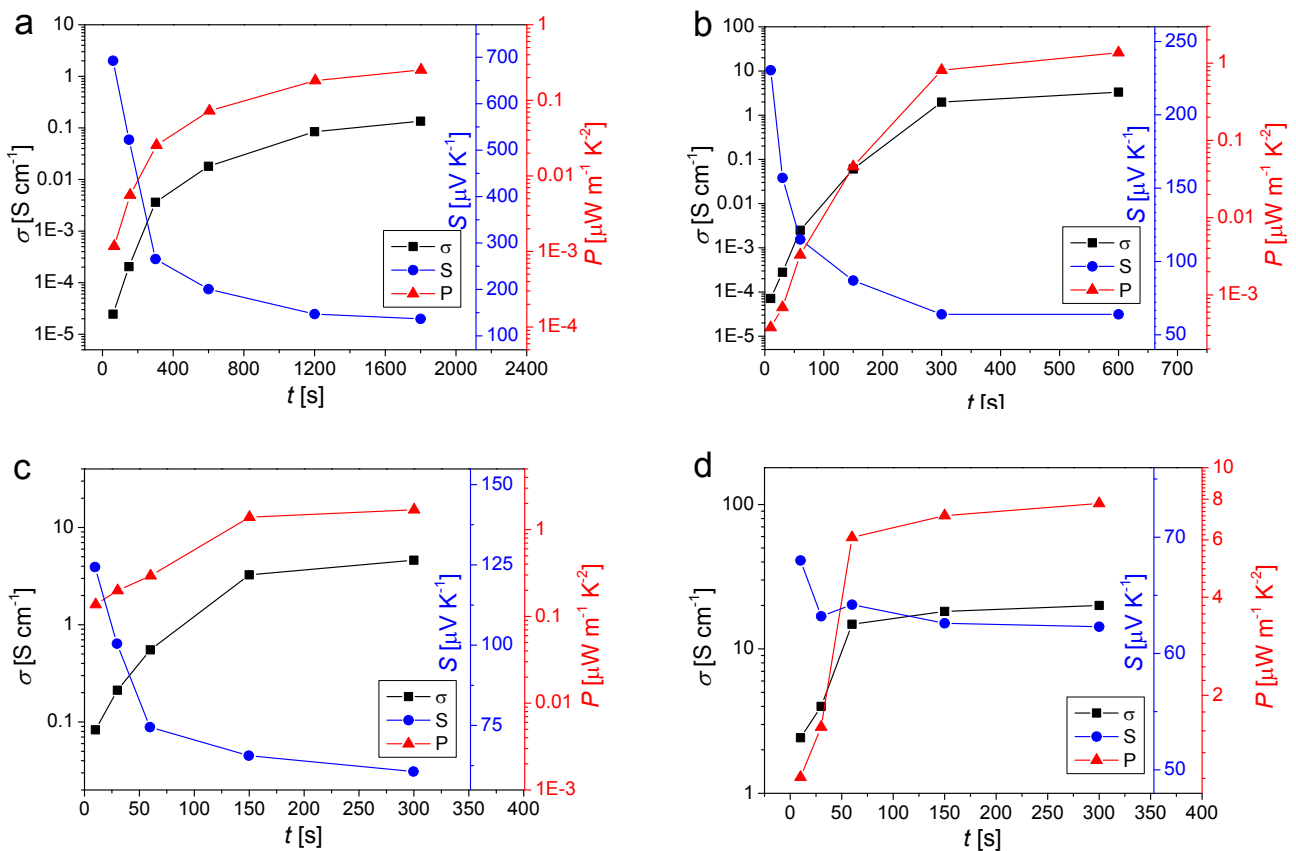


**Figure S9.** Doping level dependent thermoelectric properties of P3HT nanonet with (a) 1 mM (b) 5 mM (c) 10 mM (d) saturated (~25 mM) AgClO<sub>4</sub> concentration

Changes in the thermoelectric properties of P3HT during the doping reaction with silver cations were followed (Figure S7) using different oxidant concentrations. Results obtained at all four concentrations are shown and compared here. Generally, the observed changes follow similar pattern in all cases. Note however, that the oxidant concentration has large impact on both the kinetics and thermodynamics of the reaction. Additionally to the shorter timescale at higher concentrations, the registered, significantly higher electrical conductivities indicate higher doping level of the polymer. Best thermoelectric performance was achieved at the highest oxidant concentration, with heavily doped P3HT nanonet.

#### *Elemental composition of the silver doped P3HT nanonet*

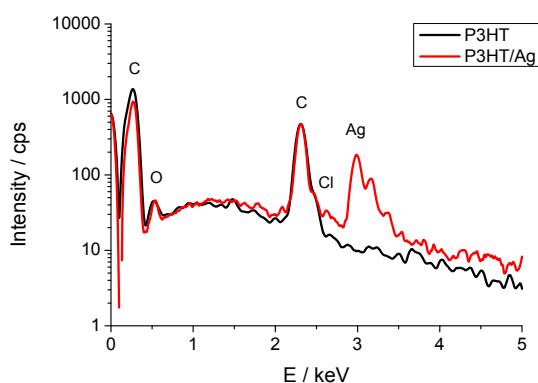
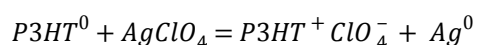


**Figure S10.** EDX spectra of the undoped and the  $\text{Ag}^+$  doped ( $[\text{AgClO}_4] \sim 25\text{mM}$ ) P3HT nanonet

After doping with the highest concentration of the oxidant, EDX analysis revealed the presence of considerable amount of silver in the P3HT nanonets. Importantly, for the bare PHT no chloride was detected by this technique, but it was clearly visible for the composite sample. Since the formation of metallic Ag (instead of silver perchlorate or silver chloride) was confirmed by XRD the proposed schematic reaction mechanism is the following:



Although EDX is considered only as a semi-quantitative method, comparison of the *relative* amounts of the different atoms shed important light on the doping procedure. From EDX data obtained for the most heavily doped sample (with  $\sim 25\text{ mM}$   $\text{Ag}^+$  concentration in the solution) the C/S ratio was found to be around 11 (theoretically 10), while a Ag/S ratio of 0.4 was obtained (the absolute value of



Ag is 3.2 mol% in this case). This latter value can be correlated to the doping level of PHT, since it gives the number of Ag<sup>+</sup>-cations reduced per each monomeric unit (note that one monomer contains one sulfur atom). Importantly, the calculated doping level (0.4) is in perfect agreement with those values reported for heavily doped PHT (see refs 24 and 25 in the m/s).

## References

- S1. H. Järvinen, L. Lahtinen, J. Näsman, O. Hormi and A. - Tammi, *Synth.Met.*, 1995, **69**, 299.
- S2. H. Werheit, U. Kuhlmann, B. Herstell and W. Winkelbauer, *Journal of Physics: Conference Series*, 2009, **176 (012037)**, 1.
- S3. N. Kiriy, E. Jähne, H. Adler, M. Schneider, A. Kiriy, G. Gorodyska, S. Minko, D. Jehnichen, P. Simon, A. A. Fokin and M. Stamm, *Nano Lett.*, 2003, **3**, 707.
- S4. W. D. Oosterbaan, V. Vrindts, S. Berson, S. Guillerez, O. Douheret, B. Ruttens, J. D'Haen, P. Adriaensens, J. Manca, L. Lutsen and D. Vanderzande, *J.Mater.Chem.*, 2009, **19**, 5424.
- S5. S. Samitsu, T. Shimomura and K. Ito, *Thin Solid Films*, 2008, **516**, 2478.
- S6. Y. Furukawa, M. Akimoto and I. Harada, *Synth.Met.*, 1987, **18**, 151.
- S7. H. Wei, L. Scudiero and H. Eilers, *Appl.Surf.Sci.*, 2009, **255**, 8593.